BMC Microbiology

Research article

The dynamic behavior of bacterial macrofibers growing with one end prevented from rotating: variation in shaft rotation along the fiber's length, and supercoil movement on a solid surface toward the constrained end

Neil H Mendelson*[1], Patrick Shipman[2], Darshan Roy[3], Liling Chen[1] and John J Thwaites[4]

Address: [1]Department of Molecular and Cellular Biology, University of Arizona, Tucson, AZ 85721, USA, [2]Department of Mathematics, University of Arizona, Tucson, AZ 85721, USA, [3]Department of Biochemistry and Molecular Biophysics, University of Arizona, Tucson, AZ 85721, USA and [4]Gonville and Caius College, Cambridge CB2 1TA, U.K

Email: Neil H Mendelson* - nhm@u.arizona.edu; Patrick Shipman - patrick@u.arizona.edu; Darshan Roy - darshan@u.arizona.edu; Liling Chen - lchen@email.arizona.edu; John J Thwaites - nhm@u.arizona.edu

* Corresponding author

Published: 16 August 2003

BMC Microbiology 2003, **3**:18

Received: 28 April 2003
Accepted: 16 August 2003

This article is available from: http://www.biomedcentral.com/1471-2180/3/18

Abstract

Background: Bacterial macrofibers twist as they grow, writhe, supercoil and wind up into plectonemic structures (helical forms the individual filaments of which cannot be taken apart without unwinding) that eventually carry loops at both of their ends. Terminal loops rotate about the axis of a fiber's shaft in contrary directions at increasing rate as the shaft elongates. Theory suggests that rotation rates should vary linearly along the length of a fiber ranging from maxima at the loop ends to zero at an intermediate point. Blocking rotation at one end of a fiber should lead to a single gradient: zero at the blocked end to maximum at the free end. We tested this conclusion by measuring directly the rotation at various distances along fiber length from the blocked end. The movement of supercoils over a solid surface was also measured in tethered macrofibers.

Results: Macrofibers that hung down from a floating wire inserted through a terminal loop grew vertically and produced small plectonemic structures by supercoiling along their length. Using these as markers for shaft rotation we observed a uniform gradient of initial rotation rates with slopes of 25.6°/min. mm. and 36.2°/min. mm. in two different fibers. Measurements of the distal tip rotation in a third fiber as a function of length showed increases proportional to increases in length with constant of proportionality 79.2 rad/mm. Another fiber tethered to the floor grew horizontally with a length-doubling time of 74 min, made contact periodically with the floor and supercoiled repeatedly. The supercoils moved over the floor toward the tether at approximately 0.06 mm/min, 4 times faster than the fiber growth rate. Over a period of 800 minutes the fiber grew to 23 mm in length and was entirely retracted back to the tether by a process involving 29 supercoils.

Conclusions: The rate at which growing bacterial macrofibers rotated about the axis of the fiber shaft measured at various locations along fibers in structures prevented from rotating at one end reveal that the rate varied linearly from zero at the blocked end to maximum at the distal end. The increasing number of twisting cells in growing fibers caused the distal end to continuously rotate faster. When the free end was intermittently prevented from rotating a torque developed which

was relieved by supercoiling. On a solid surface the supercoils moved toward the end permanently blocked from rotating as a result of supercoil rolling over the surface and the formation of new supercoils that reduced fiber length between the initial supercoil and the wire tether. All of the motions are ramifications of cell growth with twist and the highly ordered multicellular state of macrofibers.

Background

Filaments of *Bacillus subtilis*, consisting of chains of cells linked in tandem, twist as they grow, writhe, supercoil, and by repetition self-assemble into highly ordered fibers of mm in length called macrofibers [1,2]. The direction of twisting can be either left or right handed, and the degree of twist can be varied giving rise to fibers that range from very tightly twisted to those so loose that they barely retain their integrity as fibers. Helix hand and the degree of twist are both governed by genes and environmental factors such as temperature, or the presence of certain ions or compounds in the growth medium [3]. In any given culture all the fibers grow with the same handedness and degree of twist [4,5]. All fibers carry loops at both ends of the fiber shaft that rotate during growth in contrary directions about the axis of the shaft [6,8]. If the loops are removed the ends of the shaft also rotate in contrary directions. We have shown previously that the sum of the angles turned through at the ends of such fibers is a linear function of their length [8] which strongly suggests that fibers grow with constant twist, and that the rate at which a fiber shaft rotates must decrease from a maximum at the ends to zero at some point along the length of a fiber.

The presumed gradient of rotation rate along the shaft of a macrofiber has never been observed directly although pivoting motions observed as fibers grow on solid surfaces clearly show a gradient of velocity of rotation in the horizontal plane which is the result of rolling over the surface that correspondes to the rate of rotation in the fiber [7,8]. Simple theory predicts that if rotation is prevented at only one end of a fiber the other should rotate at twice the rate it normally would, and that the rotation rate should vary linearly along the shaft from zero at the blocked end to maximum at the other.

In all previous work on macrofibers it has been evident that anything that impedes fiber rotation during growth simultaneously at two locations along a fiber's length results in supercoiling in the region between the impediments [4,10]. In particular impediment to rotation at the free end of fibers blocked at their other end has previously been shown to induce supercoiling [11]. In fiber populations blocking rotation at one end of a fiber caused by fiber/fiber interactions followed later by blocking the other end has been shown to result in supercoiling and the dragging of the two ends together. The work described here deals with the characterization of the rotation rate gradient in fibers experimentally blocked at one end, as well as the ramifications of later preventing rotation at the free end of such fibers.

Results

A bacterial macrofiber was suspended in growth medium from a textile fiber which was floated on the surface. The textile fiber remained fixed in orientation on the fluid surface as the bacterial fiber grew vertically toward the floor of the chamber. Macrofiber growth was observed using a CCD video camera fitted with a telephoto lens aimed horizontally at the chamber. The optics chosen permitted visualization of the full depth (approximately 10 mm) of the growth fluid. It also allowed resolution of macrofiber details adequate to quantify the rates of fiber growth and rotation of the shaft and distal tip of the elongating structure. Time-lapse video images were produced and used to analyze these parameters for three macrofibers designated 8, 9, and 82.

Three parameters were measured in macrofibers suspended in fluid growth medium using the floating "wire" protocol: i. the length extension of the fibers as they grew, ii. the rotation of the fiber shaft at various distances from the floating wire, and iii. the rotation of the distal tip of the fiber as it elongated. The length extension as a function of time of the two fibers used to measure shaft rotation are shown in Fig. 1. Two segments are shown in the plot of length versus time for fiber number 9 reflecting a shortening in length caused by supercoiling. The slopes of both these curves and that for fiber number 8 indicate that the fibers grew exponentially with a length doubling time in the range of 82 to 83 minutes.

Supercoils that arose in hanging fibers formed short plectonemes that were used to determine the rates at which the fiber shaft rotated during growth. These markers were distributed along the length of the fibers (Fig. 2). Although the wires (textile microfilament) from which these fibers hung cannot be seen in these images, the fluid/air interface can be resolved. Consequently we measured the distance of each marker from the interface as an index of its location relative to the fixed end of the fiber. The four markers chosen in each fiber to measure shaft rotation are indicated in Fig. 2. The rotation rate of the fiber shaft at the position of each marker was determined

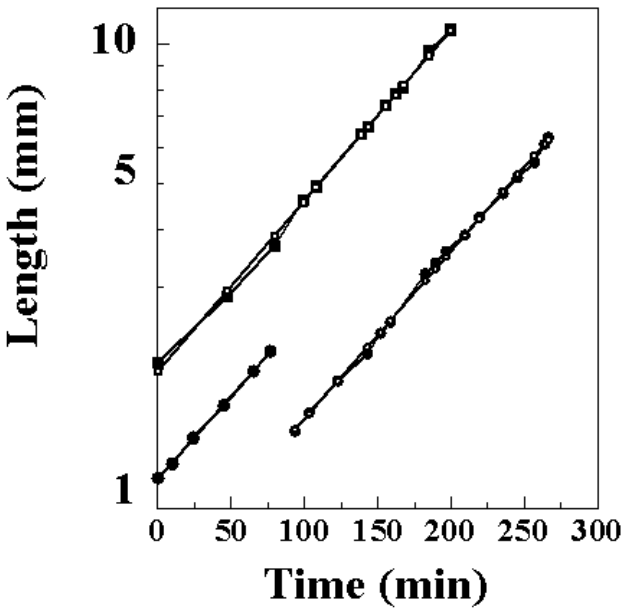

Figure 1
The growth of tethered macrofibers 8 and 9. The contour length extension as a function of time of the two right-handed macrofibers, 8 (square symbols) and 9 (circle symbols), that grew from hanging wires and were used to measure the rotation rate gradients. Closed symbols = measurements, open symbols = exponential fit of the data: correlation = 0.99.

by measuring the number of 1/2 turns as a function of time. All of the measurements shown were taken over the same time course (see Fig. 3 legend for details). Fig. 3 illustrates that markers proximal to the wire rotated more slowly than those located further from it. The rotation rates for fibers 8 and 9 as a function of distance from the wire are shown in Fig. 4. The values approximate to the initial (tangent) rates of the graphs of Fig. 3, using the first six 1/2 turns in each case. The corresponding linear fits for both sets of rates are shown. The gradient for fiber 8 is 25.6°/min. mm and for fiber 9, 36.2°/min. mm. The film images from which these data were derived can be viewed in additional files 2 and 3.

In many film sequences the distal tip of fibers grown from hanging wires can be seen to rotate at an accelerating rate as the fibers elongate. Occasionally such fibers writhed sufficiently for their distal tip to touch the fiber shaft before the fiber had grown long enough to touch the floor of the growth chamber. Whenever a fiber touches its own shaft it supercoils by a folding rather than a buckling mode. In one such case (fiber 82) the resulting supercoil gave rise to a structure at the distal tip that could be used to measure the rotation at the tip. The structure of fiber 82 prior to and after formation of the tip marker is shown in Fig. 5. Fiber 82 grew at an exponential rate prior to and after formation of the tip marker (Fig. 6). The segment of this curve for which no values are shown (120 to 320 minutes) spans the interval during which fiber 82 reorganized and produced the distal tip marker. Length measurements were not possible during this period. Rotation of the distal tip was measured over a period of approximately 65 minutes as shown in Fig. 7. The bold straight lines are linear fits to four segments of the curve. The initial rotation rate was 286°/min, the final rate was 430°/min. The open circle symbols on Fig. 7 represent a theoretical fit of rotation based upon length changes using a model described below. The inferred gradient of rotation angle vs. length is 79.2 rad/mm. Additional file 1 shows part of the film sequence used to determine the rate at which the distal tip rotated during fiber growth. One also sees in this sequence that the macrofiber eventually made contact with the floor of the chamber and could no longer rotate freely after having done so. No further measurements were made on this or other sequences described here after the macrofiber had come in contact with the floor.

In the course of other experiments in which macrofibers were prevented from rotating at both of their ends by inserting steel wires through their terminal loops and positioning the wires in contact with the floor, occasionally fibers detached from one of the two wires and continued to grow with one free end. Unlike hanging wire fibers these structures grew horizontally above the floor of the growth chamber and periodically made contact with the floor at various points throughout their growth (Fig. 8). Additional file 4 shows part of the film sequence from which the frames in Fig. 8 were taken. One sees from Fig. 8 and the film that twisting and writhing motions resulted in supercoils that moved over the floor toward the wire to which one end of the fiber was tethered. Figure 9 depicts the kinetics of fiber growth elongation and supercoil movement toward the wire tether. Each supercoil retraction to the tether reduced the length of fiber extending from the tether. Although to begin with the remaining linear portion of the fiber continued to elongate, it too underwent supercoiling and consequent shortening. The rate of supercoil movement was approximately 4 times the rate of fiber length extension so the total length of fiber, approximately 23 mm, was eventually drawn back to the tether. The end result was a massive ball-like structure surrounding the wire tether. The entire process took 800 minutes. The first 350 minutes involved fiber elongation; the remaining time involved retraction. Figure 9 shows that at later times there were multiple supercoils located at different positions along the shaft simultaneously traveling toward the tether.

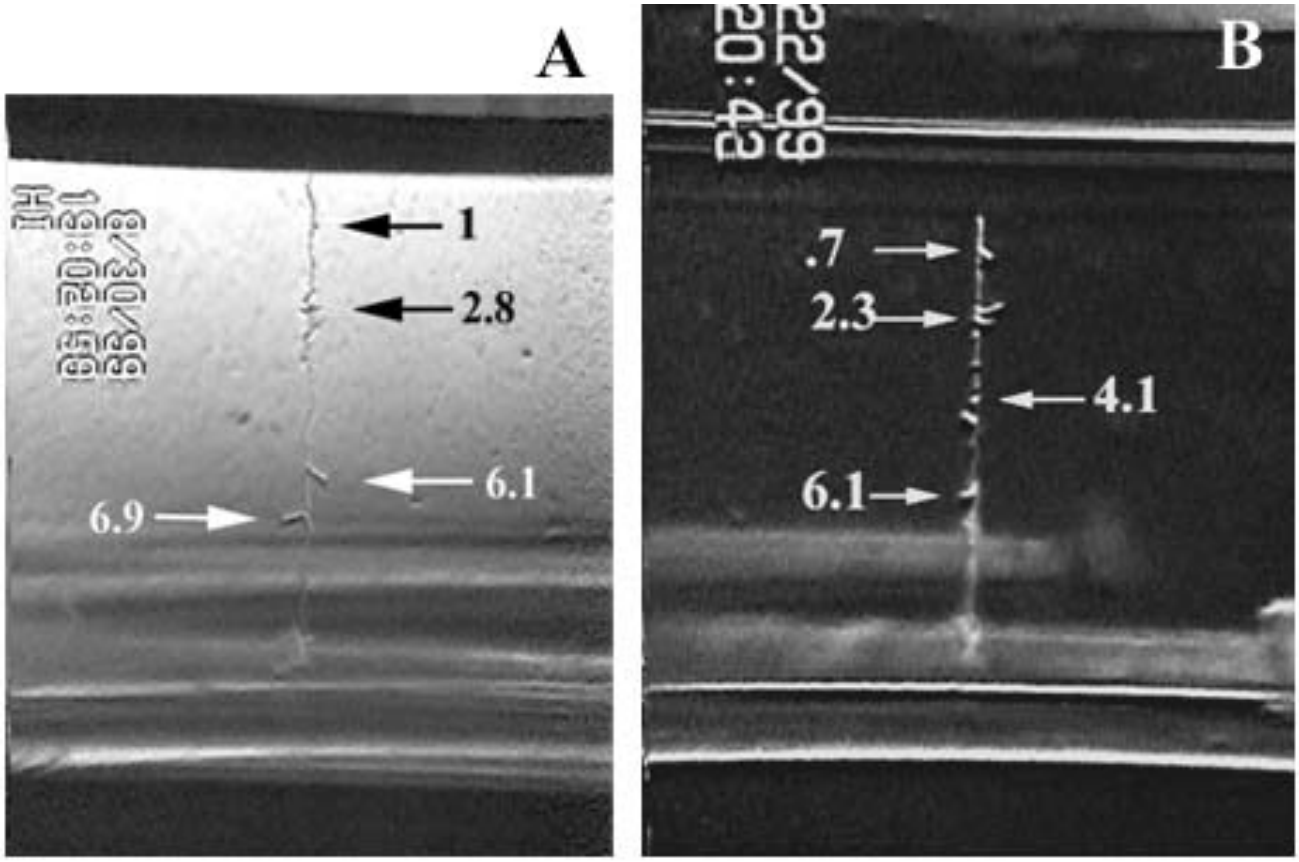

Figure 2
Micrographs of the plectoneme supercoil markers used to measure shaft rotation during growth of tethered macrofibers 8 and 9. The tether wire was located at the top of each fiber. Arrows point to the 4 markers in each fiber used to obtain rotation rates. Numbers are distances of the markers from the tether in mm. A = fiber 8, B = fiber 9.

Discussion

The experiments described here illustrate that in growing bacterial macrofibers that are tethered at one end, rotation rate gradients develop, that the rate at which the free end of a tethered fiber rotates increases as a function of fiber elongation, and that a second block to fiber rotation at a distance from the tether induces plectoneme supercoils that migrate on solid surfaces toward the tether. All of these observations can be understood in terms of the behavior of a deformable filament that twists as it elongates, and when twisting is impeded develops torque that is relieved by changing shape. Earlier work has suggested that all of the cells in a macrofiber grow, even those at its center [8]. Individual cells, and therefore macrofibers, grown without constraint expand [12], toward both poles of their approximately cylindrical structure. The methods we used to block macrofiber rotation at one end also imposed a constraint on growth expansion. The cell mass produced by growth of cells in a tethered fiber must be taken up by expansion solely toward the free end of the fiber. A similar situation arises in natural macrofiber populations when mature fibers form ball-like structures that harbor younger fibers growing outward from their surface [13]. These young fibers can neither rotate at the end attached to the ball structure as they grow, nor expand into the ball structure. Their behavior is the same as that found in the tethered fibers described here.

A single cell positioned within a macrofiber at its tethered end, unlike a free cell, can rotate as it grows only at its distal pole. The twist generated by its growth can influence only the downstream neighboring cell to which the initial cell is attached by a septum. Growth of the downstream cell is subject to the same constraints but it is also influenced by the twist generated by its upstream neighbor. This polarity continues throughout the entire fiber and is the key mechanical reason for rotation gradient behavior and the fact that the downstream tip of the fiber rotates

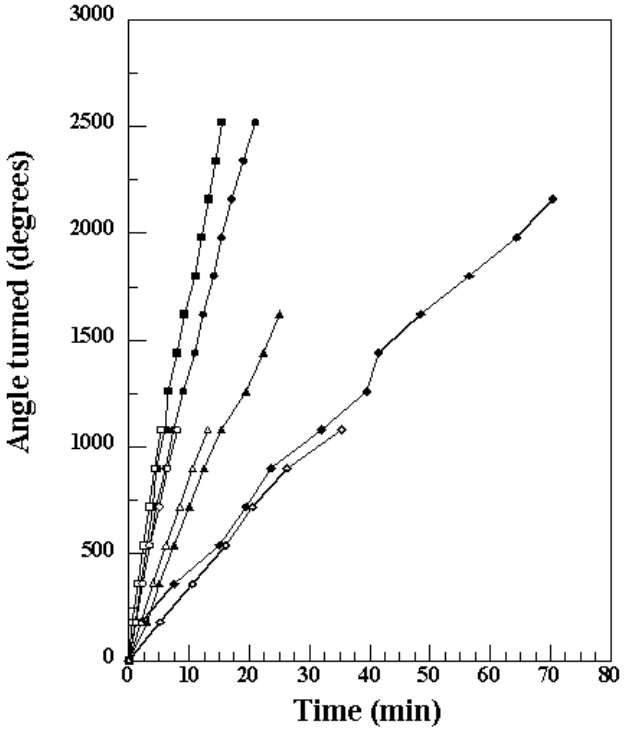

Figure 3
The rotation of plectoneme markers about the shaft of macrofibers 8 (filled symbols) and 9 (open symbols) during growth. The locations of the markers (distance from the tether in mm) were as follows: diamond symbols fiber 8 = 1, fiber 9 = 0.7; triangle symbols fiber 8 = 2.8, fiber 9 = 2.3; circle symbols fiber 8 = 6.1, fiber 9 = 4.1; square symbols fiber 8 = 6.9, fiber 9 = 6.1. The relative time shown correspond to real time as follows: for markers in fiber 8 relative time 0 for the marker at 1 mm corresponds to actual time 0, for the marker at 2.8 mm relative time 0 = actual time 9 min 48 sec, for the markers at 6.1 and 6.9 mm relative time 0 = actual time 13 min 11 sec. For markers in fiber 9 relative time 0 for the marker at 4.1 mm corresponds to actual time 0, for the marker at 6.1 mm relative time 0 = actual time 11 sec, for the markers at 0.7 and 2.3 mm relative 0 = actual time 37 sec. The actual times at which measurements began were dictated by the time when the plectoneme markers formed and became positioned so that their rotation about the fiber axis could be accurately assessed.

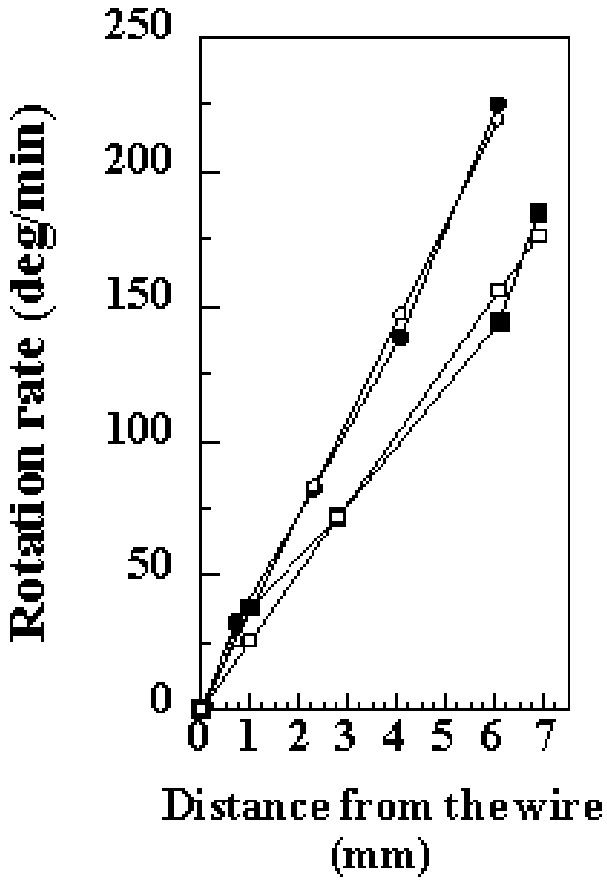

Figure 4
The rotation rate gradient as a function of distance (mm) from the tether in macrofibers 8 (square symbols) and 9 (circle symbols). Open symbols are linear fits to the data (filled symbols).

faster and faster as more cells are produced by growth all along the length of the macrofiber. We modeled mathematically the dynamic behavior of a macrofiber tethered at one end making the following simplifying assumptions: i. the macrofibers have uniform diameter throughout their length, ii. there is uniform twist throughout the fiber structure, and iii. the fibers grow at an exponential rate. The model predicts that the rotation rate at any point in a tethered fiber is proportional to the rate of growth of the segment between the tether and that point and depends solely on the fiber's twist. The argument is essentially the same for unconstrained macrofibers [8]; thus:

$$\Omega_x = 2\pi N \dot{x} \qquad (1)$$

where Ω_x is the rotation rate at length x from the tether and N is twist in turns/unit length. When the fiber growth rate is exponential (ν) as the measurements in Figs. 1 and 6 indicate it is, the relationship becomes

$$\Omega_x = 2\pi N \nu x \qquad (2)$$

where $x = x_o e^{\nu\tau}$ and $\nu = (\ln 2)/T_d$, T_d is the doubling time.

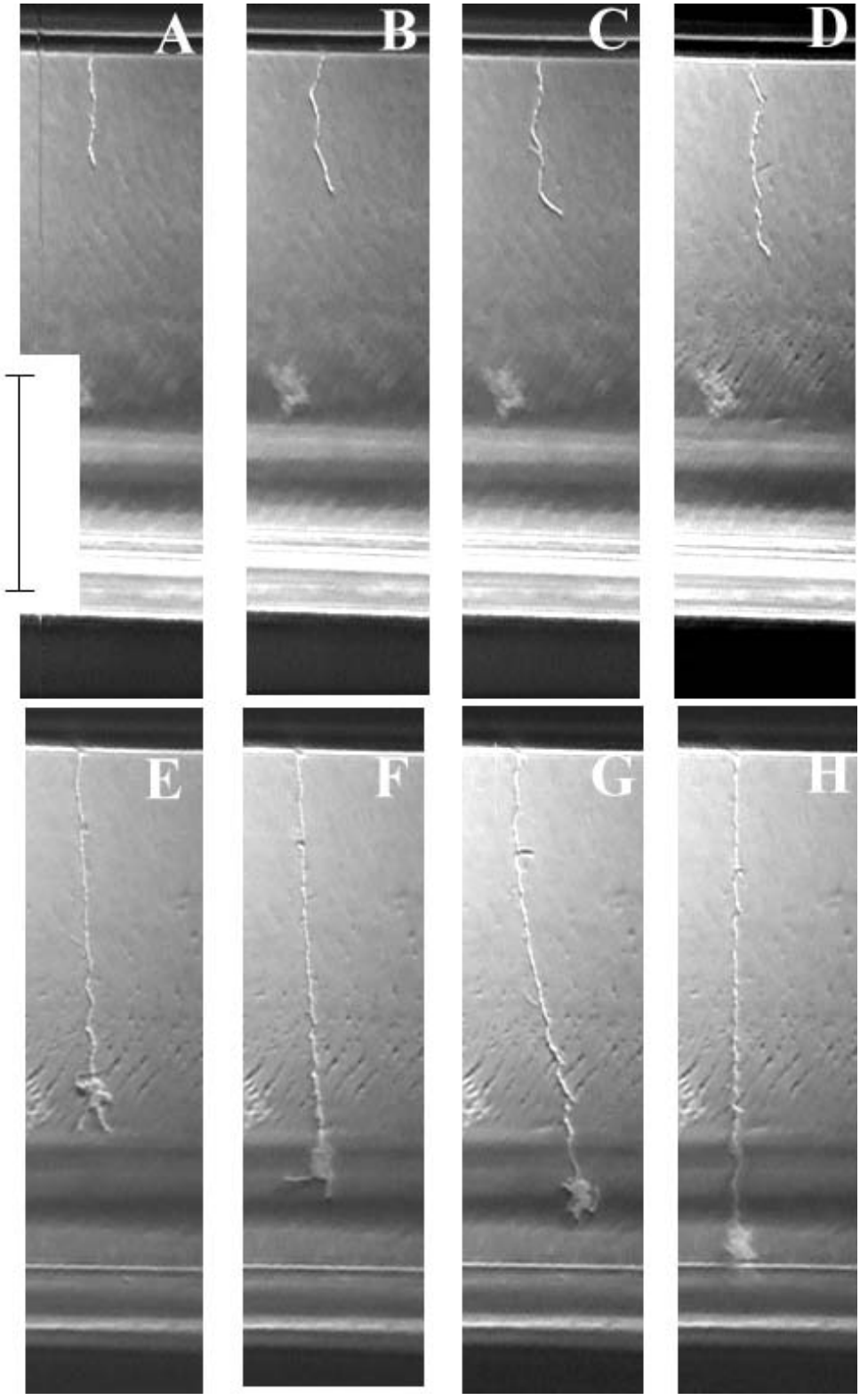

Figure 5
Micrographs showing the structure of macrofiber 82 before and after the formation of a marker at its distal tip that was used to measure tip rotation rates. The times of each frame relative to frame A are: A = 0, B = 41 min, C = 51 min, D = 60 min, E = 332 min, F = 357 min, G = 375 min, H = 398 min. Bar in frame A = 5 mm.

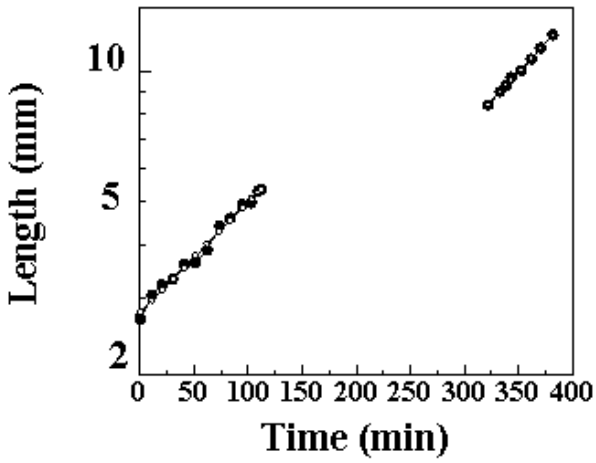

Figure 6
The growth (length extension) of macrofiber 82 as a function of time prior to and following marker formation shown in Fig. 5. Filled symbols = measured lengths, open symbols = exponential fit of the data.

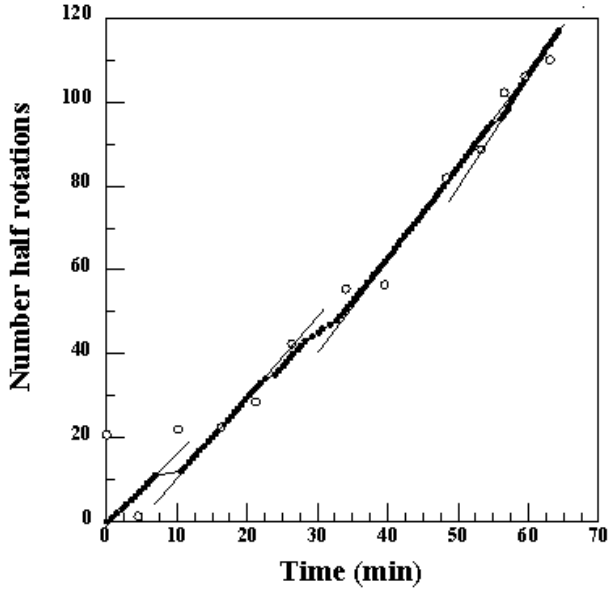

Figure 7
The rotation of the distal tip of macrofiber 82 about the shaft of the fiber as a function of growth. The time intervals between 180° rotations (filled circles) were determined from the film sequence shown in additional file 1. The straight lines were drawn by eye through points at various sections of the curve. Open symbols represent rotation derived from observed length values fit using a model described in the text.

Integrating (2) with respect to time gives the angle turned through θ

$$\theta_x = 2\pi N x_o(e^{\nu\tau} - 1) = 2\pi N(x - x_o) \qquad (3)$$

which is the form the data takes in Fig. 3 for markers along the length of the shaft and in Fig. 7 for measurements of rotation at the distal tip. Using this relationship we are able to solve for N in fiber 9 given ν = 0.0083 min^{-1}. The inferred twist is 12.1 turns/mm. The same calculation using measurements from fiber 82 (that from which distal tip rotation rate was measured) results in an inferred twist of 12.6 turns/mm. That for fiber 8 however results in a twist of only 8.7 turns/mm. All three fibers were grown under the same conditions so that a common twist value should be expected. The most likely reason for fiber 8 twist being different is that, although the plectoneme markers on fiber 9 moved away from the surface tether at a speed corresponding to the whole fiber growth rate, those on fiber 8 did so at speeds that on average were only 0.70 times the corresponding fiber growth rate. It is clear that elongation of plectonemes reduces the rate of elongation of the macrofiber shaft, but there is no simple theory relating this to rotation rate, so the fact that 8.7/12.1 = 0.71 is probably coincidence.

If we examine the film sequences shown in additional files 1, 2, and 3 all of which depict tethered macrofiber growth using the hanging wire protocol, we see that the first assumption of the model, uniform diameter throughout length, is true initially but not at later times after supercoil plectonemes arose. For technical reasons twist could not be measured directly in these fibers therefore we cannot assess the validity of the second assumption of our model. Figs 1 and 6 show that the third assumption of the model, uniform growth rate, is correct. Given these limitations we can nevertheless compare the rotation rate gradients with those predicted by our model of ideal behavior. Using the plectoneme markers shown in Figs. 2 and 5, the rates of rotation along the shaft (Figs. 3 and 4) and at the distal downstream tip (Fig. 7) were determined. In the two fibers measured the variation along the shaft of each fiber was linear (Fig. 4): in fiber 8 the gradient of rate of change as a function of distance from the tether was approximately 25.6°/min. mm, in fiber 9 it was 36.2°/min. mm.

Both fibers grew at an exponential rate. According to our simple model the rotation rate should have also increased at an exponential rate with time; but they did not. This was probably due to rotational viscous drag acting upon the macrofiber because the fiber surface moved relative to the fluid. The drag would have resulted in a torque about the longitudinal axis of the fiber. The effect of such a torque, Q is, in the simple theory given above, to reduce

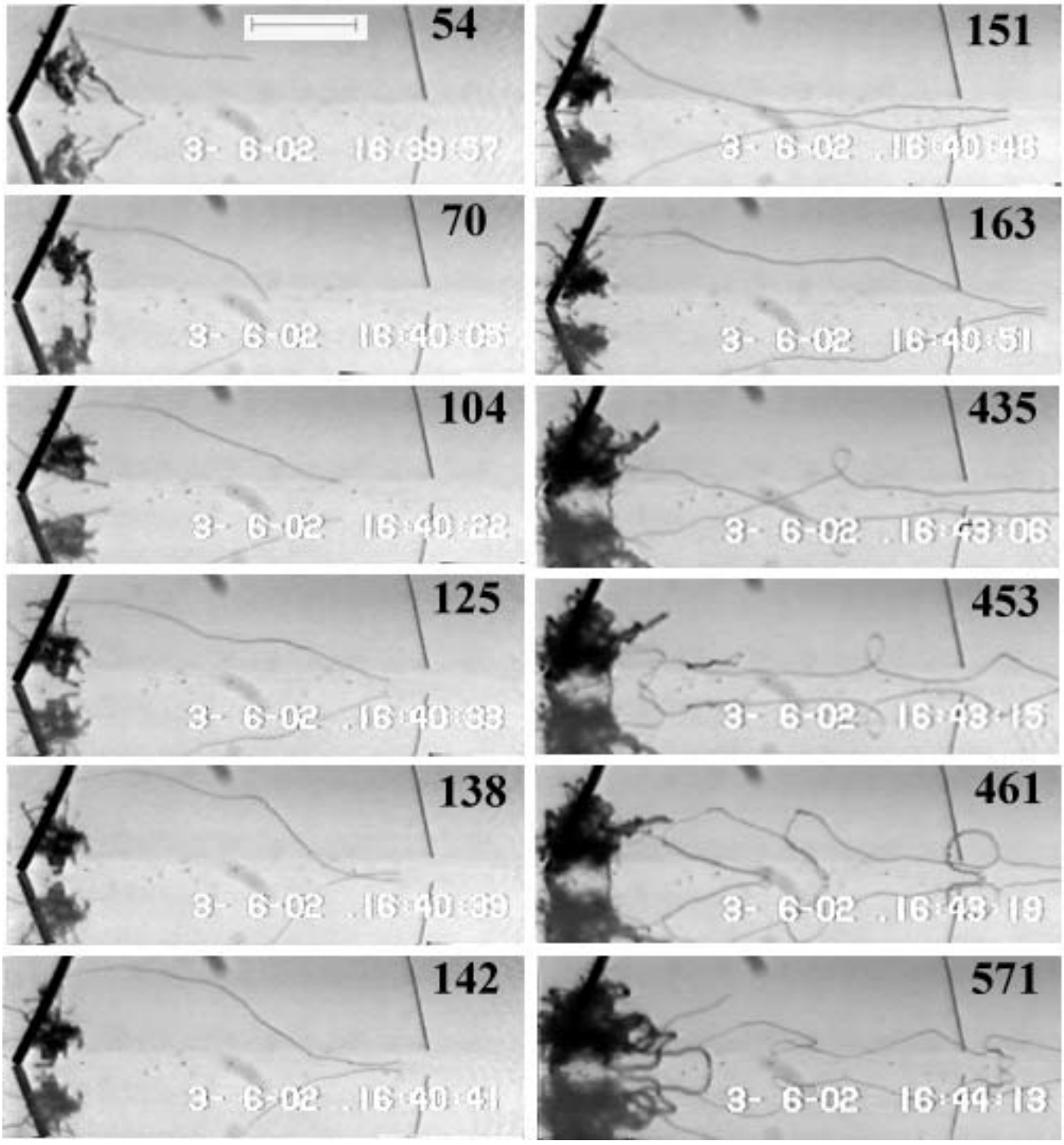

Figure 8

Images of the horizontal growth of a tethered macrofiber, its contact with the floor, supercoiling and movement of the supercoils toward the tether. The black numbers in each frame represent minutes from the start of the film sequence (white numbers were added during recopying of the sequence and should be ignored). The 12 frames are side view images taken from the sequence shown in additional file 4. The fiber was tethered to the steel wire (76 μm diameter) shown at the left of each frame. A mirror image reflection from the floor of the chamber can be seen and used to determine where the fiber is in contact with the floor. Bar = 1 mm.

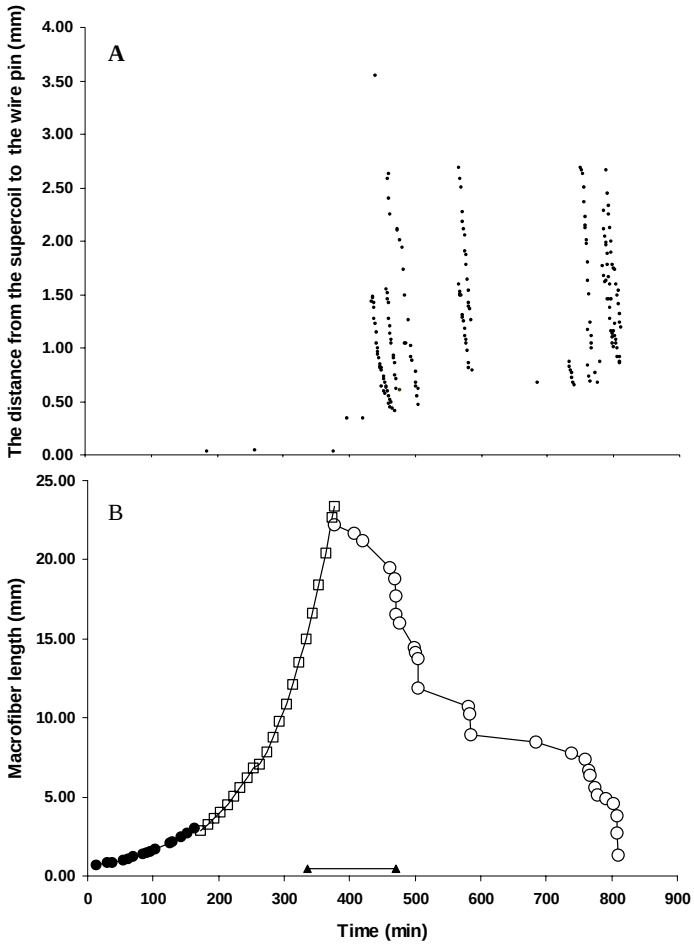

Figure 9

The growth, supercoiling and movement of the macrofiber shown in Fig. 8. Filled circles on the bottom curve (B) are measured lengths, open squares are theoretical projections of continued length extension based upon the initial growth rate. Open circles represent the calculated fiber length from the tether obtained by subtracting the length of fiber shaft shortened by its incorporation into plectoneme supercoils from the projected maximum length obtained by fiber growth. The upper curves (A) show the times at which supercoils formed and their distance from the tether. Points on the upper curve correspond to the same time axis as those on the lower curve. Points aligned beneath one another on the upper curve indicate the movement of a supercoil toward the tether. The first three supercoils arose close to the tether and therefore did not move. Later arising supercoils were prevented from moving all the way to the tether by the mass of fiber accumulated there from earlier supercoils as shown in additional file 4. (Two triangles connected with a horizontal line on panel B indicate the starting [336 minutes] and ending [472 minutes] times corresponding to the film sequence shown in additional file 4.) Preferred locations for supercoil initiation were initially at the tether, then at the surface of fiber mass attached to the tether. At later times supercoils arose at distances of approximately 1.5 and 2.6 mm from the tether. A total of 29 supercoils were observed.

the effective twist $2\pi N$ in equation (1) by an amount Q/C where C is the torsional stiffness at the point under consideration. Because of their distance from the axis of rotation, the viscous drag on plectonemes is the major cause of macrofiber torque. This then depends on rotational speed, which does increase with time, so the effective twist decreases with time resulting in a non-exponential change in rotation rates. This does not affect the variation with position; the rates used in Fig. 4 were all initial rates. Better scaling proportionality was found however for the case of distal downstream tip rotation as a function of fiber length as shown in Fig. 7. During a 65 min. interval the rotation rate of the distal tip progressively increased from an initial rate of 286°/min. to 335, then to 382, and finally to 430°/min. The transitions between these rates were rather abrupt suggesting that there may be some thresholds that have to be overcome in order for the tip to increase its rate of rotation. The geometry of the tip markers may play some role in this. Their orientation with respect to the fiber shaft changed throughout the growth period examined. During the initial 8 minutes of Fig. 7, for example, two arms protruded perpendicular to the fiber shaft at the tip. These became aligned with the axis of the shaft between 8 and 10 minutes and remained in this orientation for the period corresponding to the second linear portion of the curve suggesting that changes in the viscous drag may be a contributing factor. For the purposes of modeling tip behavior however we have ignored this complication. Our mathematical model predicts a relationship between rotation rate and fiber length of:

$$\theta_l/\pi = 25.2(l\text{-}8.66) \qquad (4)$$

(where l is length in mm). Corresponding points based upon equation (4) have been superimposed upon the data of Fig. 7. The fit appears to be good suggesting proportionality between the growth rate of an entire fiber and the rate at which it's tip rotates. Because any torque due to viscous drag depends on the length of a macrofiber and the plectonemes beyond the section concerned, it should be zero at the tip. This explains why the rotation rate at the tip of a fiber (fiber 82 for example), unlike that at intermediate points, increases, on average, exponentially.

These findings establish that blocked rotation at one end during growth of macrofibers leads to the development of rotation rate gradients in which the further away from the point of impediment one gets, the faster the structure rotates as it elongates. Earlier we have shown using a similar floating wire protocol that preventing rotation at both ends during growth leads to supercoiling [11]. In natural macrofiber populations blocked rotation usually results from contacts fibers make with the floor of the growth chamber [7]. We describe here an inadvertent discovery in which a fiber prevented from rotating at one end by tethering to a wire later became prevented from rotating at various positions along its length as a result of touching the floor. Fig. 8 and additional file 4 show that plectoneme supercoils arose following the second impediment to rotation. Fig. 9 illustrates that the newly formed plectonemes migrated over the floor toward the initial tether eventually causing the entire length of the fiber (23 mm) to retract. The formation of new supercoils in the region between the tether and the plectoneme was responsible for retraction. Film sequence 4 clearly shows that the bulky plectoneme protruding from the fiber shaft prevented free shaft rotation and induced the secondary supercoils that shortened the length of fiber shaft between the plectoneme and the tether. A similar phenomenon has been observed in natural macrofiber populations when macrofibers bridging between two larger ball form structures were caused to supercoil, reduce their length and drag the two structures together [13].

Although bacterial macrofibers respond to forces as would any comparable deformable material their mechanical behavior is unique because all forces at play are derived from individual cell growth within the multicellular fibers and because impediments to the rotation that accompanies cell elongation set into play motions that when resisted can result in work being done. Macrofibers are therefore true self-organizing micromachines. The magnitude of forces they can generate is currently being measured using special force gauges and instrumentation that will be described in another publication.

Conclusions

The ends of freely growing macrofibers rotate in contrary directions as fibers elongate. If one end of a growing fiber is prevented from rotating the dynamic behavior of the fiber is disrupted and a new set of rules govern the motions that accompany growth. Tethered fibers develop rotation rate gradients along their length; the rate ranges from zero at the tether to a maximum at the other (free) end. The magnitude of maximum rate is governed by the twist state of the fiber and the fiber length. In a fiber whose twist was inferred to be approximately 12.6 turns/mm we observed a maximum tip rotation rate of 430°/min at a fiber length of approximately 10.7 mm. In similar fibers the rotation rate gradient along the fiber shaft was found to be constant at rates in two cases of 25.6°/min. mm. and 36.2°/min. mm. Tethered fibers allowed to make contact with a solid surface that blocked rotation at various distances from the tether developed plectoneme supercoils that migrated over the solid surface toward the tether eventually causing the entire length of the fiber (23 mm) to collapse back to the tether. Similar behavior has been observed in natural populations when fibers become

tethered at one end as a result of their attachment to other structures.

Methods

Bacteria

Bacillus subtilis strain FJ7 [14] was grown as right-handed macrofibers in the standard complex medium, TB, containing magnesium using standard macrofiber culturing conditions [15].

Media and growth conditions

The complex medium, TB, consisted of 10 g Bacto Tryptose (Difco), 3 g Bacto Beef Extract (Difco) and 5 g of NaCl per L deionized water. Overnight cultures were grown at 20°C from toothpick transfer of fragmented mature fibers into fresh TB containing 50 mM $MgSO_4$ [14]. For hanging wire experiments the most uniform young and short macrofibers that carried a loop at one end large enough so that a wire could be inserted into it were selected from the populations and transferred into fresh medium of the same composition housed in a plastic chamber. The chamber was fabricated from an 85 × 22 × 45 mm (length, width, height) disposable tissue culture bottle by removing 20 mm of its height. Polyester textile microfilaments, 23 μm in diameter and 1 to 2 mm in length, were used to block terminal loop rotation. They were inserted by hand into a terminal loop and floated on the surface of the growth medium. The macrofibers hung down into the solution. The growth chamber was positioned on a glass plate, illuminated with diffuse fluorescent light from behind, and incubated at 24°C. The experiment involving horizontal growth of a tethered macrofiber near the floor of a growth chamber utilized a glass chamber, 56 × 25 × 13 mm (length, width, height). A 76 μm diameter stainless steel wire (Cal Fine wire) was inserted into the loop at one end of the fiber using a precision motorized micromanipulator (MP-285, Sutter Instrument Co., CA) and lowered to touch the floor of the glass chamber. Initially the opposite end of the fiber was tethered to a 10 μm diameter stainless steel wire designed to act as a force transducer. The transducer was raised above the glass surface to allow its movement in response to supercoiling but the fiber slid off the end of the wire before measurements could be taken. The fiber collapsed down in a supercoil onto the larger wire tether at its other end. The observations described in this paper began after the fiber grew out from cell mass clumped on the large wire tether. The tether remained in place throughout the the experiment.

Video film production and analysis

In the hanging wire experiments images of growth and motions were obtained using a Cohu charge-coupled device camera fitted with a Fujinon TV zoom lens (1/12 175/75 mm) to which Tiffen closeup lenses were added. The video images were written on VHS tape with a JVC time lapse tape deck prior to transfer to a PC via a Matrox frame grabber and Matrox Inspector software (Matrox Graphics, Montreal). Image analysis was done using the Image Pro Plus program (Media Cybernetics). Dual-view images of the macrofiber that grew horizontally above the floor of the growth chamber were captured using two Hitachi (Hitachi Denshi, Ltd.) charge-coupled device cameras fitted to Navitar optical tubes. Both images were sent to a Phase Eight screen splitter (Vicon Industries). The synchronized output was then routed to a GYYR time-lapse tape deck (Odetics). Both images were recorded simultaneously on the same film and a date and time stamp was printed on each frame. All figures were assembled using the Adobe Photoshop program (Adobe Systems). Graphs were constructed using Microsoft Excel (Microsoft Corporation). Curve fitting was done using the Psi Plot program (Poly Software International).

Authors' contributions

NM designed the protocols for hanging wire and two wire experiments, designed the optical system for gathering images and the system used for their processing and analysis. He also measured and analyzed the rotation rate data. PS conducted the hanging wire experiments. DR conducted the two wire experiment from which the supercoil migration data were obtained. LC measured length elongation rates, analyzed the supercoil migration data and contributed to computer analysis of other findings. JT developed the mathematical models and guided the interpretation of results in terms of mechanics.

Additional material

Additional File 1

Time-lapse video film sequence of tethered macrofiber number 82. The fiber hung from a floating wire above and grew toward the floor of the growth chamber below. The rotation of the distal tip was measured using the projecting plectoneme arms that protrude from the mass at the tip. Other plectonemes can be seen rotating about the fiber's shaft during growth. The entire sequence spans about 120 min in real time.
Click here for file
[http://www.biomedcentral.com/content/supplementary/1471-2180-3-18-S1.mov]

Additional File 2

Time-lapse video film sequence of tethered macrofiber number 8. (See additional file 1 for details.) The formation, elongation and rotation of plectoneme markers used to measure shaft rotation can be seen. The entire sequence spans about 180 min. in real time.
Click here for file
[http://www.biomedcentral.com/content/supplementary/1471-2180-3-18-S2.mov]

Additional File 3

Time-lapse video film sequence of tethered macrofiber number 9. (See additional files 1 and 2 for details.) The entire sequence spans about 130 min. in real time.
Click here for file
[http://www.biomedcentral.com/content/supplementary/1471-2180-3-18-S3.mov]

Additional File 4

Time-lapse dual-view video film sequence of a tethered macrofiber growing horizontally above the floor of the growth chamber. The upper image is the view from above and is not pertinent to this analysis. The lower image shows the view from the side including a mirror image reflection of the fiber from the glass floor. The fiber grew from the large mass attached to the wire at the left toward the right of the field of view. Writhing motions, supercoiling, and supercoil movement toward the left can be seen in the lower images. The entire sequence spans 136 minutes in real time. The initial frame of this sequence corresponds to 336 min on Fig. 9. For purposes of orientation two triangles and a connecting horizontal line drawn on panel B of figure 9 indicate where the starting and ending time frames are of additional file 4 in the context of the entire growth and retraction process.
Click here for file
[http://www.biomedcentral.com/content/supplementary/1471-2180-3-18-S4.mov]

Acknowledgements

This work was supported by a grant from the National Center for Research Resources, NIH to NHM. D.R. and P.S. were supported by the University of Arizona Undergraduate Biology Research Program. We thank Elissa Reptowitz for help in organizing the video film libraries and providing indices for rapid location of particular sequences, and Michael Wagenheim for processing video film images for internet use.

References

1. Mendelson NH: **Helical *Bacillus subtilis* macrofibers: morphogenesis of a bacterial multicellular macroorganism.** *Proc Natl Acad Sci USA* 1978, **75:**2478-2482.
2. Mendelson NH: **Self-assembly of bacterial macrofibers: a system based upon hierarchies of helices.** *Mat Res Soc Symp Proc* 1992, **255:**43-54.
3. Mendelson NH: **Regulation of *Bacillus subtilis* macrofiber twist development by D-cycloserine.** *J Bacteriol* 1988, **170:**2336-2343.
4. Mendelson NH: **Helical growth of *Bacillus subtilis:* a new model of cell growth.** *Proc Natl Acad Sci USA* 1976, **73:**1740-1744.
5. Briehl MH and Mendelson NH: **Helix hand fidelity in *Bacillus subtilis* macrofibers after spheroplast regeneration.** *J Bacteriol* 1987, **169:**5838-5840.
6. Mendelson NH: **Bacterial growth and division: genes, structures, forces and clocks.** *Microbiol Revs* 1982, **46:**341-375.
7. Mendelson NH, Sarlls JE and Thwaites JJ: **Motion caused by the growth of *Bacillus subtilis* macrofibres in fluid medium result in new forms of movement of the multicellular structures over solid surfaces.** *Microbiol* 2001, **147:**929-937.
8. Mendelson NH and Thwaites JJ: **Twisted states of *Bacillus subtilis* macrofibers reflect structural states of the cell wall.** *Proc Natl Acad Sci USA* 1984, **81:**3562-3566.
9. Mendelson NH, Sarlls JE, Wolgemuth CW and Goldstein RE: **Chiral self-propulsion of growing bacterial macrofibers on a solid surface.** *Phys Rev Lett* 2000, **84:**1627-1630.
10. Mendelson NH and Thwaites JJ: **Bending, folding, and buckling processes during bacterial macrofiber morphogenesis.** *Mat Res Soc Symp Proc* 1990, **174:**171-178.
11. Mendelson NH: ***Bacillus subtilis* macrofibers, colonies and bioconvection patterns use different strategies to achieve multicellular organization.** *Environ Microbiol* 1999, **1:**471-477.
12. Mendelson NH, Thwaites JJ, Kessler JO and Li C: **Mechanics of bacterial macrofiber initiation.** *J Bacteriol* 1995, **177:**7060-7069.
13. Mendelson NH, Morales D and Thwaites JJ: **The mechanisms responsible for 2-dimensional pattern formation in bacterial macrofiber populations grown on solid surfaces: fiber joining and the creation of exclusion zones.** *BMC Microbiology* 2002, **2:**1.
14. Fein JE: **Helical growth and macrofiber formation in *Bacillus subtilis* 168 autolytic enzyme deficient mutants.** *Can J Microbiol* 1980, **26:**330-337.
15. Mendelson NH and Favre D: **Regulation of *Bacillus subtilis* macrofiber twist development by ions: effects of magnesium and ammonium.** *J Bacteriol* 1987, **169:**519-525.